Gating TrkB switch by methylglyoxal enables GLO1 as a target for depression

Ziyin Wu[1,2,3]†, Yingxue Fu[2,3]†, Yinfeng Yang[3,4]†, Chao Huang[2,3]†, Chunli Zheng[1,3]†, Zihu Guo[1,3]†, Zihao Yang[6], Xuetong Chen[2,3], Jinglin Zhu[1,3], Jinghui Wang[4], Xiaogang Li[1,3], Liyang Chen[2,3], Weiwei Zhou[3,5], Yangyang Chen[2,3], Jiangmei Wang[2,3], Yang Yang[3,5], Meng Jiang[1,3], Sushing Chen[7], Aiping Lu[8], Jianlin Liu[1], Yan Li[4], Shiguo Sun[6], Zhenzhong Wang[3], Wei Xiao[3]*, Yonghua Wang[1,3]*

[1]Lab of Systems Pharmacology, College of Life Sciences, Northwest University, Xi'an, Shaanxi 710069, China.

[2]Center of Bioinformatics, College of Life Sciences, Northwest A&F University, Yangling, Shaanxi 712100, China.

[3]State Key Laboratory of New-tech for Chinese Medicine Pharmaceutical Process, Lianyungang, Jiangsu 222001, China.

[4]Key Laboratory of Industrial Ecology and Environmental Engineering (MOE), Department of Materials Sciences and Chemical Engineering, Dalian University of Technology, Dalian, Liaoning 116024, China.

[5]Pharmacology department, School of Pharmacy, Shihezi University, Shihezi 832002, China.

[6]Shaanxi Key Laboratory of Natural Products & Chemical Biology, College of Chemistry & Pharmacy, Northwest A&F University, Yangling, Shaanxi 712100, China.

[7]Systems Biology Laboratory, Department of Computer Information Science and Engineering, University of Florida, Gainesville, Florida, United States of America.

[8]School of Chinese Medicine, Hong Kong Baptist University, Kowloon Tong, Hong Kong.

†These authors contributed equally to this work.

*Correspondence should be addressed to Yonghua Wang (yhwang@nwu.edu.cn) and Wei Xiao (xw_kanion@163.com).

Abstract

Major depressive disorder (MDD) is a severe psychiatric illness that affects about 16 percent of the global population. Despite massive efforts, unravelling the pathophysiology of MDD and developing effective treatments is still a huge challenge. Here, we report a novel therapeutic axis of methylglyoxal (MGO)/tropomyosin receptor kinase B (TrkB) for treating MDD. As an endogenous metabolite, MGO was demonstrated directly binding to the extracellular domain of TrkB, provoking its dimerization and autophosphorylation. This rapidly enhances the expression of brain-derived neurotrophic factor (BDNF) and forms a BDNF-positive feedback loop. Low-dose treatment of MGO effectively promotes the hippocampal neurogenesis and exhibits sustained antidepressant effects in chronic unpredictable mild stress rat models. In addition, the modulation on MGO concentration by overexpression or inhibition of Glyoxalase 1 (GLO1) has been demonstrated associated with depression behaviors in rats. Furthermore, we also identified a natural product luteolin and its derivative lutD as potent inhibitors of GLO1 and explored their precise binding modes. Our findings reveal a novel regulatory mechanism underlying MDD and depict principles for the rational design of new antidepressants targeting GLO1.

Significance Statement

Methylglyoxal (MGO) is an endogenous reactive dicarbonyl metabolite which is often involved in disease conditions by reacting with cellular components and causing oxidative stress. While high concentrations of MGO exert toxicity resulting in aging and diabetic neuropathy, we here find that MGO levels are remarkedly decreased in depression rats, and low-dose MGO treatment alleviates depression-like symptoms and promotes the hippocampal neurogenesis. This unexpected effect is achieved by MGO's modification of TrkB and the subsequent activation of downstream Akt/CREB signaling, which leads to a rapid and sustained expression of BDNF. The antidepressant role of endogenous MGO provides a new basis for the design of therapeutic interventions for major depressive disorder.

Key Words

Depression; Methylglyoxal; BDNF/TrkB signaling; Hippocampal neurogenesis; Antidepressant

Introduction

Major depressive disorder (MDD) is a common, devastating illness associated with serious health and socioeconomic consequences (1). Increasing evidence has associated this disease with impairments in the brain-derived neurotrophic factor (BDNF) signaling pathway which regulate neuronal survival and synaptic plasticity (2, 3). BDNF is an important member of the neurotrophin family, which binds to the tropomyosin receptor kinase B (TrkB) (4) to regulate neuronal proliferation and differentiation in the nervous system (5-7). In MDD patients, the expression of BDNF in the prefrontal cortex (PFC) and hippocampus (HC), as well as in the plasma, is markedly decreased (6, 8). One cause for the reduced BDNF levels is due to BDNF/TrkB signaling dysfunction mediated by endogenous small molecules, such as the N-methyl-D-aspartate (NMDA) (9). However, whether there are other endogenous metabolic molecules involved in regulating BDNF/TrkB signaling under depressive state is still largely unknown.

Methylglyoxal (MGO) is an endogenous metabolite mainly generated in the glycolysis process (10). It is a highly reactive dicarbonyl aldehyde, which can react with protein arginine and/or lysine residues to form advanced glycation end-products (AGEs), and cause non-enzymatic, post-translational modifications of proteins (11, 12). High concentrations of MGO exert cytotoxic effects via evoking the production of reactive oxygen species (13), and have been implicated in pathologies of several diseases including diabetes (14), aging (15) and neurodegenerative diseases (16). Nevertheless, under normal conditions, MGO can be efficiently detoxified by the glyoxalase system, mainly through Glyoxalase 1 (GLO1), an enzyme catalyzing the conversion of acyclic α-oxoaldehydes to corresponding α-hydroxyacids (17). Recently, GLO1 has been identified associated with anxiety- and depression-like behaviors in mice (18, 19). This suggests that MGO may play a potential role in the pathophysiology of depression. However, the cellular function of MGO at physiological concentration and its precise mechanism of action in depression still remain poorly understood.

In this study, we report that MGO functions as an endogenous agonist of TrkB by directly binding to its extracellular domain (ECD) to stimulate its dimerization and autophosphorylation. This enables MGO to switch on the BDNF/TrkB signaling, manipulating a fast and sustained activation effect through forming a BDNF-positive feedback loop. We further demonstrate that MGO can effectively promote the hippocampal neurogenesis and exhibit antidepressant effects in chronic unpredictable mild stress (CUMS) rat model. Moreover, we have screened out a natural product luteolin, which selectively binds to GLO1 and exerts desirable antidepressant effects. Further, the key residues of the binding pocket between luteolin and GLO1, i.e., E99, F62 and Q33 were determined.

Results

GLO1 has negative regulation effects on BDNF/TrkB signaling pathway.

To systematically identify those genes that are associated with MDD, we performed a differential coexpression analysis on a publicly available gene expression profiling of brain samples from 34 MDD

patients and 55 normal individuals (GSE45642) (**Supplementary Fig. S1*A***) (20). Firstly, the differentially coexpressed genes (DCGs) of six brain areas, i.e., the dorsolateral PFC (DLPFC), anterior cingulate cortex (AnCg), HC, amygdala (AMY), nucleus accumbens (NAcc) and cerebellum (CB) were obtained using an improved weighted correlation network analysis (I-WGCNA) approach (21) (see Methods, **Supplementary Table S1**). Pathway enrichment analysis of the six DCG sets against KEGG database identified the 'neurotrophin signaling pathway' as one of the most significantly enriched pathways in the DLPFC, AnCg, HC and NAcc areas (**Supplementary Fig. S1*B***). Then, by employing the gene set enrichment analysis (GSEA) algorithm, a panel of genes like NGF and BDNF were identified associating with this pathway, which is consistent with their neurotrophic roles (22). Notably, among them, a homodimeric zinc metalloenzyme GLO1 was found significantly correlated with the BDNF/TrkB signaling pathway in the DLPFC, HC, NAcc and CB areas of these samples (**Fig. 1*A* and Supplementary Fig. S1*C***). All analyses raise an interesting assumption that GLO1 may be involved in regulating the BDNF/TrkB signaling in the DLPFC, HC and NAcc areas of MDD patients.

To test this, two independent, non-overlapping short hairpin RNA (shRNA) lentiviral constructs were designed to knock down GLO1 in PC12 cells (**Supplementary Table S2**). The levels of GLO1 protein and its mRNA were significantly down-regulated in both of the shRNA groups (**Figs. 1*B* and 1*D***). We then tested whether this knockdown impacts the signaling transduction of BDNF/TrkB pathway. The results show that the expression levels of BDNF protein and its mRNA were both obviously enhanced (**Figs. 1*C* and 1*D***). Correspondingly, silencing of GLO1 increased the levels of p-TrkB, p-Akt, p-ERK1/2 and p-CREB (**Fig. 1*E***), indicating the activation of Akt and ERK signaling pathways, which are important downstream signals that regulate the neuronal survival and local axon growth (23). Additionally, the pharmacological inhibition of GLO1 by 10 μM S-p-bromobenzylglutathione cyclopentyl diester (BBGC) in WT PC12 cells also resulted in an enhancement of TrkB signaling (**Supplementary Fig. S2*A***). Reciprocally, the overexpression of GLO1 in PC12 cells significantly increased both the protein and mRNA levels of GLO1 (**Fig. 1*F*** and **Supplementary Fig. S2*B***). And this led to a reduction of p-TrkB, p-Akt, p-ERK1/2 and p-CREB levels, as well as the protein and mRNA levels of BDNF (**Figs. 1*G*, 1*H*** and **Supplementary Fig. S2*B***), indicating that GLO1 overexpression causes functional inhibition of BDNF/TrkB signaling. All these data strongly support the speculation that GLO1 has negative regulation effects on BDNF/TrkB signaling pathway.

MGO functions as a TrkB agonist and induces a fast and sustained BDNF/TrkB signaling.

Considering that the concentrations of MGO can be controlled by GLO1 (10), and GLO1 negatively regulates the BDNF/TrkB signaling, we hypothesize that MGO may positively modulate this signaling pathway, and in this way increase the expression of BDNF. To validate this, we first measured the concentrations of MGO in PC12 cells after silencing or inhibiting GLO1 and found a significant increase in MGO concentrations when compared to the control (**Supplementary Figs. S3*A* and S3*B***). In contrast, when GLO1 was overexpressed, the intracellular MGO levels were significantly decreased in the transfected cells (**Supplementary Fig. S3*C***). These results confirm that the concentrations of MGO are inversely proportional to GLO1 enzymatic activity (24).

We further investigated whether MGO regulates the phosphorylation levels of TrkB and its

downstream effectors. As expected, incubation of MGO with PC12 cells for 1 h produced a concentration-dependent activation of the TrkB signaling pathway (**Supplementary Fig. S3*F***). Consistently, MGO also increased the expression of BDNF mRNA in a dose-dependent manner (**Supplementary Fig. S3*D***). Furthermore, incubation of MGO at 250 μM for 15 or 30 min both robustly increased the levels of p-TrkB, p-Akt, p-ERK1/2 and p-CREB (**Supplementary Fig. S3*G***), which demonstrates that MGO provokes the activation of BDNF/TrkB signaling in a fast way. Importantly, the nuclear entry of p-CREB was also significantly promoted by 250 μM MGO (**Supplementary Fig. S4*D***) and the mRNA levels of BDNF robustly increased at 3 h, peaked at 12 h and was detectable until 24 h, which is consistent to its changes at the protein level (**Supplementary Fig. S3*E* and S4*A***). Besides, the phosphorylation of TrkB and the downstream p-ERK1/2 and p-CREB stimulated by 250 μM MGO can last up to 12 h (**Supplementary Fig. S4*A***). This long-lasting BDNF/TrkB signaling induced by MGO may enhance the synaptic transmission in adult hippocampus, and thus lead to antidepressant-like effects (25, 26).

Next, we explored the molecular mechanisms underlying this fast and sustained activation effect of MGO on BDNF/TrkB signaling. Firstly, to exclude the activation effects due to the accumulation of BDNF, we added the BDNF antibody to the cell cultures and found that it only partly abrogated MGO-induced phosphorylation of Akt, ERK1/2 and CREB in the first 9 h (**Fig. 2*A*** and **Supplementary Fig. S4*B***). This result suggests that the apparent signaling activation effect caused by MGO does not completely attribute to BDNF. Further, we utilized K252a, a potent selective inhibitor for Trk receptors (27), to investigate whether MGO's effect is associated with the kinase activity of TrkB. As shown in Fig. 2e, K252a potently inhibited the phosphorylation of TrkB, Akt and ERK1/2 that was stimulated by BDNF or 7,8-dihydroxyflavone (7,8-DHF), a known small molecule agonist of TrkB (28). And the levels of p-TrkB, p-Akt and p-ERK1/2 induced by 250 μM exogenous MGO or 10 μM BBGC were also significantly decreased by this inhibitor (**Fig. 2*B*** and **Supplementary Fig. S4*C***). Additionally, K252a also decreased the p-CREB levels and its nuclear entry induced by MGO (**Figs. 2*B*, 2*C*** and **Supplementary Fig. S4*D***). All these demonstrate that the biological function of MGO is closely associated with the kinase activity of TrkB.

Further, the pull-down assays showed that treatment of 250 μM MGO or 100 ng/mL BDNF significantly provoked the homodimerization and autophosphorylation of TrkB (**Fig. 2*D***), which indicates that MGO physiologically mimics the functions of BDNF. The biolayer interferometry (BLI) assay showed that MGO directly binds to the extracellular domain (ECD, 32-429aa) of TrkB with a dissociation constant (K_d) of 5.31 μM (**Fig. 2*E***). However, MGO does not interact with the intracellular domain (ICD, 454-821aa) of TrkB (**Supplementary Fig. S4*E***). This finding is important because in this way MGO generated in cytoplasm can rapidly diffuse across the cell membrane to enter into the extracellular space to bind to TrkB (18), avoiding potential intracellular off-target effects. Taken in sum, MGO selectively binds to the ECD of TrkB and functions as its agonist, and thus induces a fast and sustained activation of BDNF/TrkB signaling.

MGO promotes the hippocampal neurogenesis and presents antidepressant effects on depression rats.

Increasing BDNF expression is essential for the antidepressant action of both conventional antidepressants and the fast-acting agents, like ketamine (29, 30). Since MGO exhibits the capability of

enhancing the expression of BDNF *in vitro*, we further investigated whether MGO also exerts this effect *in vivo* which then leads to antidepressant activity (**Supplementary Fig. S5*A***). We found that the treatment of low-dose MGO (5 mM/kg per day) for 3 weeks significantly reduced the immobility time of CUMS rats in the forced swim test (FST) (**Fig. 3*A***) and robustly increased their time in the open arms in the elevated plus-maze (EPM) (**Fig. 3*B*** and **Supplementary Fig. S5*B***). Consistently, the protein levels of GLO1 were significantly up-regulated in both HC and PFC areas of CUMS rats when compared with controls, whereas low-dose MGO treatment slightly decreased its expression levels but not significantly (**Fig. 3*D* and Supplementary Fig. S6*A***). Besides, an acute high dose treatment of MGO (50 mM/kg per day, ip) for 3 days also exhibited desirable antidepressant effects (**Supplementary Fig. S5*C***). These suggest that MGO produces both sustained and fast-acting antidepressant effects on CUMS rats.

Next, we analyzed the levels of neurotransmitters in HC and PFC of rats, as the reduction of neurotransmitters in brain is a major contributing factor to depression (31). LC-MS/MS analysis showed that the concentrations of 5-HT, DA, 5-HIAA, DOPAC and HVA were significantly decreased in HC and PFC of CUMS rats (**Fig. 3*C*** and **Supplementary Fig. S6*B***). But ip injection of low-dose MGO greatly increased the levels of these neurotransmitters in the brain of CUMS rats (**Fig. 3*C*** and **Supplementary Fig. S6*B***), implying that the augmentation of the neurotransmitters is necessary for the antidepression function of MGO.

We further examined whether in the brains of CUMS rats MGO activates the BDNF/TrkB signaling pathway. It is observed that the concentrations of MGO in both HC and PFC areas, as well as the plasma of CUMS rats were significantly decreased, whereas low-dose treatment of MGO for 3 weeks recovered MGO levels back to normal concentrations (**Fig. 3*E*** and **Supplementary Fig. S6*C***). Coinciding with this, low-dose MGO treatment significantly provoked the phosphorylation of TrkB and increased the levels of p-Akt, p-ERK1/2 and p-CREB in both HC and PFC areas of CUMS rats (**Fig. 3*F*** and **Supplementary Fig. S6*D***). And this led to a significantly increased expression and release of BDNF in both of these brain areas (**Fig. 3*F* and Supplementary Fig. S6*D***). More importantly, we also found that after a single acute treatment of MGO (100 mM/kg) to CUMS rats, the TrkB signaling pathway in HC maintained a persistent activation state in 9 h (**Supplementary Fig. S6*E***), which is consistent with MGO's long-lasting effects on BDNF/TrkB signaling in PC12 cells (**Fig. 2*C***). All these demonstrate that MGO triggers the activation of BDNF/TrkB signaling in both HC and PFC areas of CUMS rats.

Further, to explore the biological effects of MGO-stimulated BDNF/TrkB signaling on CUMS rats, we conducted an RNA sequencing analysis on the HC and PFC areas of CUMS rats treated with either vehicle or 100 mM/kg MGO. Pathway enrichment analysis of the differentially expressed genes (DEGs) in PFC identified the 'neurotrophin signaling pathway' as the top-ranked KEGG pathway (**Supplementary Tables S4, S5** and **Supplementary Fig. S6*G***). Functional enrichment analysis of these DEGs showed that they mainly participated in the proliferation and differentiation of neurons (**Fig. 3*G***), which is responsible for maintaining the neuron development and neurogenesis in the adult brain (32). Consistently, qRT-PCR analysis further validated that MGO significantly up-regulated the mRNA expression levels of Cnot7, Ptgs2 and Rela that are involved in the positive regulation of cell proliferation, and down-regulated Cav2, Btg1 and Tob1 that are responsible for the negative regulation of cell proliferation (**Fig. 3*H*** and **Supplementary Table S5**). In addition, MGO also increased the mRNA expression levels of Bdnf, Rps6ka2 and Abl1, which

are important genes in the BDNF/TrkB signaling (**Fig. 3*H*** and **Supplementary Table S5**). These findings indicate that the activation of BDNF/TrkB signaling by MGO results in mainly a positive regulation of the neuron proliferation.

Accumulating evidence has suggested that altered neurogenesis in adult hippocampus mediates the action of antidepressants (33). Thus, we further examined whether MGO is able to modulate hippocampal neurogenesis. It is observed that the density of both BrdU+ new born neurons and BrdU+/NeuN+ neurons was decreased in the hippocampal dentate gyrus (DG) of CUMS rats (**Fig. 3*I***). Whereas low-dose MGO treatment significantly increased the proportion of these cells (**Fig. 3*I***), indicating that MGO is capable of promoting hippocampal neurogenesis in CUMS rats. Together, all these demonstrate that MGO effectively promotes the hippocampal neurogenesis by activating the BDNF/TrkB signaling pathway, and thus presents antidepressant effects in CUMS rats.

Luteolin exerts antidepressant effects by targeting GLO1.

The desirable antidepressant effects of MGO makes GLO1 a potential therapeutic target for depression. Firstly, to demonstrate the association between GLO1 and depression-like behaviors in rats, we utilized the adeno-associated viral (AAV) vector-mediated overexpression of GLO1 in the HC of rats. The results showed that OE-GLO1 rats exhibited a reduction of MGO concentrations in brain tissues, and a significantly increased immobility time in FST and decreased entries into open arms in EPM (**Supplementary Figs. S7*A*, *B* and *C***), which is consistent with the effects exhibited in transgenic GLO1 overexpression mice (19). Then, by application of two in house systems pharmacology-based drug targeting tools, i.e., WES (34) and TCMSP (35), a flavone molecule, luteolin, was screened out as a candidate compound that may target GLO1 (**Fig. 4*A***). The fluorescence spectroscopy experiment showed a K_d value of 47.17 μM for luteolin binding to GLO1 (**Fig. 4*B***). Additionally, the *in vivo* cellular thermal shift assay (CETSA) (36) also validates their binding in intact cells (**Fig. 4*C***) with the EC_{50} concentration of 45.23 μM for luteolin at which half-maximal thermal stabilization of GLO1 in PC12 cells was observed (**Supplementary Fig. S7*E***).

Next, to explore the binding mode of luteolin with GLO1, we performed molecular docking coupled with molecular dynamic (MD) simulations. Three residues, E99, Q33 and F62 were identified as crucial residues for the binding, as that in GLO1 active pocket they formed hydrogen bonds and an edge-to-face aromatic interaction with luteolin (**Fig. 4*D***). Then the drug affinity responsive target stability (DARTS) analysis (37) was performed with the purified GLO1 wild type or mutants (E99A, F62A and Q33E) incubated with luteolin. Resultantly, consistent with the *in silico* predictions, all mutants exhibited reduced binding affinities of luteolin to GLO1 in different extent (**Fig. 4*E***), confirming the importance of these residues in the binding pocket. Regarding luteolin, its carbonyl, resorcinol and pyrocatechol substituents form H-bonds and hydrophobic-interactions with GLO1, demonstrating the key roles of these groups in luteolin's binding within the active site of GLO1 (**Fig. 4*D***). More importantly, we found that the hydroxyl group of the resorcinol is freely buried into the positively charged mouth, a big hydrophobic tunnel constituted by residues F62, F67, L69 and T101 (**Fig. 4*D*** and **Supplementary Fig. S7*F***). To further investigate whether this hydrophobic cavity is beneficial for the binding, we modified the hydroxyl group of

the resorcinol into a bulkier group, i.e., 1, 2-dimethoxyethane, and obtained a new derivative, named as lutD (**Fig. 4*A*** and **Supplementary Fig. S8**). Intriguingly, fluorescence spectroscopy analysis presents a 1.5-fold increase of the association constant (K_a) (from 2.12×10^4 L·mol^{-1} to 3.22×10^4 L·mol^{-1}) for lutD compared with luteolin (**Supplementary Figs. S7*D***), indicating that the bulky groups in resorcinol contribute to a more potent GLO1 binding. Actually, MD simulations on lutD and GLO1 shows that this mouth zone is empty and thus provides sufficient space for bulky substituents (**Supplementary Figs. S7*F* and *G***). Besides, the hydrophobic interaction between the methoxyethane group of lutD and F67, L160 (**Supplementary Fig. S7*G***) also strengthens the interactions between lutD and GLO1. All these results demonstrate that luteolin is a potent binder of GLO1, in which H-bonds and hydrophobic interactions are important for the binding.

We next evaluated whether luteolin exhibits antidepressant effects on CUMS rats. The results show that ip administration of 10 mg/kg luteolin per day for 3 weeks markedly reduced the immobility time of rats in FST and increased their number of entries in the open arms in EPM (**Figs. 4*F*, 4*G***, and **Supplementary Fig. S9*A***). Whereas no significant effects were observed for luteolin in GLO1 overexpression rats. We also found that chronic luteolin treatment increased the plasma MGO levels and the concentrations of neurotransmitters in HC and PFC areas of rats (**Figs. 4*H*** and **Supplementary Fig. S9*B* and *C***). These results demonstrate that luteolin exerts antidepressant effects on CUMS rats by targeting GLO1. Besides, similar to MGO, luteolin treatment also promoted hippocampal neurogenesis as indicated by obviously increased number of BrdU+ or BrdU+/NeuN+ cells in the hippocampal DG of CUMS rats (**Supplementary Fig. S9*D***). Additionally, single dose treatment of 20 mg/kg luteolin potently activated the BDNF/TrkB signaling in a time-dependent manner in the HC of CUMS rats (**Fig. 4*I***). All these data reveal that through targeting GLO1, luteolin increases MGO concentrations in CUMS rats and subsequently triggers the BDNF/TrkB signaling pathway, resulting in desirable antidepressant effects.

Discussion

The present study demonstrates a novel, fast-acting MGO/TrkB axis and highlights the potential of GLO1 as a depression target (**Fig. 5**). And based on this, luteolin, as a novel GLO1 inhibitor, was discovered and its binding affinity as well as the interaction features with GLO1 were deeply explored. As a natural flavonoid, luteolin exists in many plants with antioxidant, memory-improving, and anxiolytic activities (38). Importantly, the ip lethal doses (LD_{50}) of luteolin in rats is 411 mg/kg (39), implying that it has little or no toxicity when administrated at low-dose (10 mg/kg). Therefore, this work not only presents a novel strategy for the treatment of MDD and but also identifies a natural product luteolin as a promising antidepressant.

One of our key findings is that MGO functions as an endogenous agonist of TrkB. We demonstrate that MGO directly and selectively binds to the extracellular domain of TrkB and stimulates its dimerization and autophosphorylation. And in this way, it triggers a rapid and sustained activation of TrkB-mediated Akt/CREB signaling, which rapidly increases the expression of BDNF, thus being beneficial to MDD. Clinically, increasing the BDNF level in brain is of particular therapeutic interests for depression (30, 40). However, current clinical trials using recombinant BDNF in patients always turn out disappointing due to

series of reasons like poor delivery, short half-life, and potential side effects (41). Our finding that MGO at normal concentrations acts as a switch on activating the BDNF-feedback loop provides a new feasible way to increase the BDNF levels for MDD patients. Besides, the chronic administration of MGO does not cause any weight gains in rats (data not shown), avoiding the major side effects produced by current clinically-used tricyclic antidepressants and monoamine oxidase inhibitors (42, 43). Thus, manipulating endogenous MGO concentrations in brain provides a novel alternative way for treating MDD with more favorable tolerability and efficacy.

Although several studies have suggested the potential role of GLO1 in human psychiatric disorders and its associations with depression-like behaviors (44-46), the direct evidence of the correlations between GLO1 and behavior phenotype is still lacking. The present study offers compelling evidence that GLO1 is responsible for the depression-like behaviors in CUMS rats. Importantly, we have carefully explored the druggability of GLO1. Molecular docking and MD simulations identified three residues E99, F62 and Q33 of GLO1 as key components in stabilizing the drug binding conformation, and *in vitro* mutation studies further validate the crucial roles of these amino acids. Specifically, comparing the binding pockets of luteolin and lutD to GLO1 suggests that introduction of a bulkier and negatively ionizable group at the resorcinol of luteolin can increase its hydrophobic interactions with GLO1, which produces a functionally closed gate in the protein, and strengthens the drug-target interactions. Overall, these findings highlight the possibility of GLO1 as a potential depression therapeutic target and provide important clues on how to design new antidepressants.

Materials and methods

Drugs. The following drugs were used in this study, including methylglyoxal solution (Sigma-Aldrich, M0252), S-p-bromobenzylglutathione cyclopentyl diester (Sigma-Aldrich, cat. no. SML1306), K252a (Abcam, cat. no. ab120419), luteolin (TCI chemicals, TT2682), 7,8-dihydroxyflavone (7,8-DHF) (Abcam, cat. no. ab120996), and recombinant human BDNF protein (R&D Systems, cat. no. 248-BD-025).

Animals and drug treatments. Adult Sprague-Dawley (SD) male rats (180 - 200 g) were group-housed with standard laboratory bedding and conditions (12-h light/dark cycle, 22 ± 1°C, ad libitum access to food and water) for 1 week prior to the experiments. All rats were randomly assigned to three experimental groups, i.e., non-stress control + saline (SAL); stress (CUMS) + SAL; stress (CUMS) + drugs (5 mM/kg/day of MGO or 10 mg/kg/day of luteolin). To avoid the possible bias induced by the behavioral tests, the rats in each group were divided into two sets (n = 10 per set). The first set provided tissue samples used for morphological analysis, western blotting and qRT-PCR analyses, while the second one was adopted for behavioral assessments. During the last 3 weeks of the CUMS protocol, rats were injected ip daily with drugs. The experimental procedures performed in this study were in line with the Guidelines of NIH for the Use of Laboratory Animals as well as approved by the Northwest University Animal Care and Use Committees.

CUMS. To induce the physical, behavioral, biochemical, and physiological phenotypes of depression, all rats were subjected to a schedule of mild psychosocial stressors for 8 weeks (**Supplementary Fig. S5*A***). The stressors included alterations of the bedding (sawdust change, removal or damp of sawdust, substitution of sawdust with 21°C water, rat, or cat feces), cage-tilting (45°) or shaking (2 × 30 s), cage exchange (rats were positioned in the empty cage of another male), predator sounds (for 15 min), and alterations of the length and time of light/dark cycle. Physical changes were assessed weekly by measuring the body weight of the animal. Additionally, in order to evaluate the neurogenesis by immunocytochemistry, rats were ip injected with BrdU (2 × 150 mg/kg) at the day before treatments.

Behavioral assessment. At the end of the CUMS protocol, the behavioral tests EPM and FST were conducted. Two days were given for rats between exposures to different behavioral assessments and all behavioral testing experiments were carried out during the daily light phase (09:00 am – 05:00 pm).

Elevated plus-maze test Rats were placed in the center of a standard EPM apparatus (two open and two closed 33 cm × 5 cm arms) for examining the anxiety-like behaviors of rats. The exploratory activity was measured over a 5-min period. Then, the percentage of time spent in the open arms, an index of anxiety-like behavior, the number of entries in the closed arms, an indicator of locomotion, were determined.

Forced swim test In brief, SD rats were placed in a glass cylinder filled with water (23°C; 30 cm deep) and a 5-min swim test session was video-recorded. Employing an automated video tracking system, the time spent immobile during the last 4 minutes of the test and the latency to immobility were scored. An increase in immobility time indicates a higher degree of depressive state. All tests were analyzed by TopScan (CleverSys, Inc., CSI) system.

Quantification of MGO levels. Following the manufacturers's instructions, analysis of the levels of MGO in the plasma (Hycult Biotech, HIT503) and cell lysis (Cell Biolabs, STA-811) was carried out using specific enzyme-linked immunosorbent assays. Plasma was collected from aortaventralis and separated into Eppendorf tubes that contained EDTA to inhibit coagulation effect. The mixed blood and EDTA were then inversed and placed on ice for 20 min. After the inversion, the mixture blood sample was centrifuged for 15 min at 1500×g at 4°C. The supernatant was then collected and transferred to a fresh polypropylene tube for analysis. To detect MGO-adducts in cell lysate, 50 μg of total protein from fresh tissues or cell cultures were prepared using a Qproteome Mammalian Protein Prep Kit (Qiagen, Germany) in accordance with the manufacturer's protocol.

Biolayer interferometry. The kinetics of MGO binding to the extracellular or cytoplasmic domain of recombinant human TrkB protein was assessed using biolayer interferometry with an Octet K2 system (ForteBio). All of the experiments were performed at 30°C under buffer conditions of PBST (0.1% Tween 20), pH 7.4, 8% DMSO. NI-NTA biosensors (FortéBio Inc., Menlo Park, CA) were used to capture TrkB proteins onto the surface of the sensor. After reaching baseline, sensors were moved to association step

for 60 s and then dissociated for 60 s. Curves were corrected by a double-referencing technique, using both NI-NTA pins dipped into the experimental wells and a buffer-only reference. After double referencing corrections, the subtracted binding interference data were applied to the calculations of binding constants using the FORTEBIO analysis software (Version: 9.0.0.10) provided with the instrument.

Statistical analyses. All data given in text and figures indicate mean ± s.e.m. For analysis of experiments with two groups, we used the parametric unpaired two-tailed Student's t test. For analysis of experiments with three or more groups, the parametric one-way ANOVA with Post hoc Dunnett's multiple comparisons test or two-way ANOVA with Post hoc Sidak's multiple comparisons test were used. Differences were considered significant when P was < 0.05. NS = not significant, * P < 0.05, ** P < 0.01, *** P < 0.001.

Additional materials and methods are provided in the SI Materials and Methods.

Acknowledgements

We thank Z. Jun for technical assistances and reagents. The research is financially supported by the National Natural Science Foundation of China (NO. U1603285)

Conflict of interest

The authors declare that they have no conflict of interest.

Supplementary information is available at the publisher's website.

References

1. Zanos P, *et al.* (2016) NMDAR inhibition-independent antidepressant actions of ketamine metabolites. *Nature* 533(7604):481-486.
2. Duman RS, Aghajanian GK, Sanacora G, & Krystal JH (2016) Synaptic plasticity and depression: new insights from stress and rapid-acting antidepressants. *Nat Med* 22(3):238-249.
3. Egeland M, Zunszain PA, & Pariante CM (2015) Molecular mechanisms in the regulation of adult neurogenesis during stress. *Nat Rev Neurosci* 16(4):189-200.
4. Longo FM & Massa SM (2013) Small-molecule modulation of neurotrophin receptors: a strategy for the treatment of neurological disease. *Nat Rev Drug Discov* 12(7):507-525.
5. Tuvikene J, Pruunsild P, Orav E, Esvald EE, & Timmusk T (2016) AP-1 Transcription Factors Mediate BDNF-Positive Feedback Loop in Cortical Neurons. *J Neurosci* 36(4):1290-1305.
6. Nagahara AH & Tuszynski MH (2011) Potential therapeutic uses of BDNF in neurological and psychiatric disorders. *Nat Rev Drug Discov* 10(3):209-219.
7. Castren E & Antila H (2017) Neuronal plasticity and neurotrophic factors in drug responses. *Mol Psychiatry* 22(8):1085-1095.
8. Bus BA, *et al.* (2015) Chronic depression is associated with a pronounced decrease in serum brain-derived neurotrophic factor over time. *Mol Psychiatry* 20(5):602-608.
9. Harward SC, *et al.* (2016) Autocrine BDNF-TrkB signalling within a single dendritic spine. *Nature* 538(7623):99-103.
10. Allaman I, Belanger M, & Magistretti PJ (2015) Methylglyoxal, the dark side of glycolysis. *Front Neurosci* 9:23.
11. Shamsi FA, Partal A, Sady C, Glomb MA, & Nagaraj RH (1998) Immunological evidence for methylglyoxal-derived modifications in vivo. Determination of antigenic epitopes. *J Biol Chem* 273(12):6928-6936.
12. Yao D, *et al.* (2007) High glucose increases angiopoietin-2 transcription in microvascular endothelial cells through methylglyoxal modification of mSin3A. *J Biol Chem* 282(42):31038-31045.
13. Di Loreto S, *et al.* (2004) Methylglyoxal induces oxidative stress-dependent cell injury and up-regulation of interleukin-1beta and nerve growth factor in cultured hippocampal neuronal cells. *Brain Res* 1006(2):157-167.
14. Bierhaus A, *et al.* (2012) Methylglyoxal modification of Nav1.8 facilitates nociceptive neuron firing and causes hyperalgesia in diabetic neuropathy. *Nat Med* 18(6):926-933.
15. Ramasamy R, Yan SF, & Schmidt AM (2006) Methylglyoxal comes of AGE. *Cell* 124(2):258-260.
16. Angeloni C, *et al.* (2015) Neuroprotective effect of sulforaphane against methylglyoxal cytotoxicity. *Chem Res Toxicol* 28(6):1234-1245.
17. Belanger M, *et al.* (2011) Role of the glyoxalase system in astrocyte-mediated neuroprotection. *J Neurosci* 31(50):18338-18352.
18. Distler MG, *et al.* (2012) Glyoxalase 1 increases anxiety by reducing GABAA receptor agonist methylglyoxal. *J Clin Invest* 122(6):2306-2315.
19. McMurray KMJ, *et al.* (2018) Identification of a novel, fast-acting GABAergic antidepressant. *Mol Psychiatry* 23(2):384-391.
20. Li JZ, *et al.* (2013) Circadian patterns of gene expression in the human brain and disruption in major depressive disorder. *Proc Natl Acad Sci U S A* 110(24):9950-9955.
21. Liu BH, *et al.* (2010) DCGL: an R package for identifying differentially coexpressed genes and links from gene expression microarray data. *Bioinformatics* 26(20):2637-2638.
22. Bramham CR & Messaoudi E (2005) BDNF function in adult synaptic plasticity: the synaptic consolidation

hypothesis. *Prog Neurobiol* 76(2):99-125.

23. Atwal JK, Massie B, Miller FD, & Kaplan DR (2000) The TrkB-Shc site signals neuronal survival and local axon growth via MEK and P13-kinase. *Neuron* 27(2):265-277.
24. Thornalley PJ (1996) Pharmacology of methylglyoxal: formation, modification of proteins and nucleic acids, and enzymatic detoxification--a role in pathogenesis and antiproliferative chemotherapy. *Gen Pharmacol* 27(4):565-573.
25. Kang H & Schuman EM (1995) Long-lasting neurotrophin-induced enhancement of synaptic transmission in the adult hippocampus. *Science* 267(5204):1658-1662.
26. Hoshaw BA, Malberg JE, & Lucki I (2005) Central administration of IGF-I and BDNF leads to long-lasting antidepressant-like effects. *Brain Res* 1037(1-2):204-208.
27. Tapley P, Lamballe F, & Barbacid M (1992) K252a is a selective inhibitor of the tyrosine protein kinase activity of the trk family of oncogenes and neurotrophin receptors. *Oncogene* 7(2):371-381.
28. Jang SW, *et al.* (2010) A selective TrkB agonist with potent neurotrophic activities by 7,8-dihydroxyflavone. *Proc Natl Acad Sci U S A* 107(6):2687-2692.
29. Bjorkholm C & Monteggia LM (2016) BDNF - a key transducer of antidepressant effects. *Neuropharmacology* 102:72-79.
30. Kato T, *et al.* (2017) BDNF release and signaling are required for the antidepressant actions of GLYX-13. *Mol Psychiatry*.
31. Duman RS & Aghajanian GK (2012) Synaptic dysfunction in depression: potential therapeutic targets. *Science* 338(6103):68-72.
32. Jones KR, Farinas I, Backus C, & Reichardt LF (1994) Targeted disruption of the BDNF gene perturbs brain and sensory neuron development but not motor neuron development. *Cell* 76(6):989-999.
33. Oh YS, *et al.* (2013) SMARCA3, a chromatin-remodeling factor, is required for p11-dependent antidepressant action. *Cell* 152(4):831-843.
34. Zheng C, *et al.* (2015) Large-scale Direct Targeting for Drug Repositioning and Discovery. *Sci Rep* 5:11970.
35. Ru J, *et al.* (2014) TCMSP: a database of systems pharmacology for drug discovery from herbal medicines. *J Cheminform* 6:13.
36. Jafari R, *et al.* (2014) The cellular thermal shift assay for evaluating drug target interactions in cells. *Nat Protoc* 9(9):2100-2122.
37. Lomenick B, *et al.* (2009) Target identification using drug affinity responsive target stability (DARTS). *Proc Natl Acad Sci U S A* 106(51):21984-21989.
38. Ishisaka M, *et al.* (2011) Luteolin shows an antidepressant-like effect via suppressing endoplasmic reticulum stress. *Biol Pharm Bull* 34(9):1481-1486.
39. Seelinger G, Merfort I, & Schempp CM (2008) Anti-oxidant, anti-inflammatory and anti-allergic activities of luteolin. *Planta Med* 74(14):1667-1677.
40. Ma Z, *et al.* (2017) TrkB dependent adult hippocampal progenitor differentiation mediates sustained ketamine antidepressant response. *Nat Commun* 8(1):1668.
41. Colle R, *et al.* (2015) BDNF/TRKB/P75NTR polymorphisms and their consequences on antidepressant efficacy in depressed patients. *Pharmacogenomics* 16(9):997-1013.
42. Fava M (2000) Weight gain and antidepressants. *J Clin Psychiatry* 61 Suppl 11:37-41.
43. Kent JM (2000) SNaRIs, NaSSAs, and NaRIs: new agents for the treatment of depression. *Lancet* 355(9207):911-918.
44. Benton CS, *et al.* (2012) Evaluating genetic markers and neurobiochemical analytes for fluoxetine response using a panel of mouse inbred strains. *Psychopharmacology (Berl)* 221(2):297-315.

45. Yang Y, *et al.* (2013) Proteomics reveals energy and glutathione metabolic dysregulation in the prefrontal cortex of a rat model of depression. *Neuroscience* 247:191-200.

46. Patki G, Solanki N, Atrooz F, Allam F, & Salim S (2013) Depression, anxiety-like behavior and memory impairment are associated with increased oxidative stress and inflammation in a rat model of social stress. *Brain Res* 1539:73-86.

Figure legends

Figure 1. GLO1 negatively regulates the BDNF/TrkB signaling pathway. (***A***) GSEA analysis between GLO1 coexpression gene signatures and the BDNF/TrkB signaling pathway in HC and DLPFC areas of depression patients. HC, hippocampus; DLPFC, dorsolateral prefrontal cortex. (***B*** and ***C***) Immunoblot analysis of protein expressions of (***B***) GLO1 and (***C***) BDNF (percentage of protein to GAPDH) in PC12 cells after shRNA-mediated GLO1 knockdown (shA and shB) compared to shCont. Representative western blots are shown on top of the quantitative plots. shCont, a non-targeting control shRNA; shA and shB are the shRNAs targeting GLO1. (***D***) Measurement of mRNA expression levels of GLO1 and BDNF by qRT-PCR in PC12 cells after shRNA-mediated GLO1 knockdown compared to shCont. Data are presented as mean ± s.e.m., n = 3 samples collected independently. *P < 0.05, **P < 0.01, ***P < 0.001; one-way ANOVA with Dunnett's multiple comparisons test. (***E***) Immunoblot analysis and quantification of protein expression, which highlights the increase of p-TrkB, p-Akt, p-ERK1/2 and p-CREB (percentage of phosphorylated protein to total protein) after shRNA-mediated GLO1 knockdown. Data in ***B***, ***C***, ***E*** are presented as mean percentage ± s.e.m. of the mean values of the control group; n = 3 samples collected independently. *P < 0.05, **P < 0.01, ***P < 0.001; one-way ANOVA with Dunnett's multiple comparisons test. (***F*** and ***G***) Immunoblot analysis and quantification of protein expression, which highlight the increase of GLO1 (***F***) and decrease of BDNF (***G***) protein levels (percentage of protein to GAPDH) after pHBLV-CMV-MCS-3flag-EF1 vector-mediated GLO1 overexpression. Representative western blots are shown on top of the quantitative plots. (***H***) Immunoblot analysis and quantification of protein expression, which shows the reduction of p-TrkB, p-Akt, p-ERK1/2 and p-CREB (percentage of phosphorylated protein to total protein) after lentiviral (LV) vector-mediated overexpression of GLO1 (OE-GLO1) compared with control vector (OE-Cont). Data in ***F***, ***G***, ***H*** are presented as mean percentage ± s.e.m. of the mean values of the control group, n = 3 samples collected independently. *P < 0.05, **P < 0.01; two-tailed paired t-test.

Figure 2. MGO induces a fast and sustained BDNF/TrkB signaling by binding to TrkB. (***A***) Either 250 μM MGO or additional 20 ng/mL anti-BDNF were preincubated for various periods of time with cultured PC12 cells. Representative western blots of p-CREB (S133) and CREB are shown in the left. The quantification of ratios of immunoreactivity of p-CREB (S133) to CREB is shown in the right. Data are presented as mean percentage ± s.e.m. of the mean values of the control group; n = 3 samples collected independently. *P < 0.05, **P < 0.01, ***P < 0.001, NS = not significant; two-way ANOVA with Sidak's multiple comparisons test between MGO+Anti-BDNF group and MGO group. (***B***) Preincubating PC12 cells with 10 μM 7,8-DHF, 100 ng/mL BDNF, 250 μM MGO or 10 μM BBGC for 1 h significantly activated the TrkB signaling compared to that with 1% DMSO. While addition of 100 nM K252a markedly reduced the activation effects (n = 3). (***C***) Immunocytochemistry (ICC) assay depicting the total CREB (green) and the phosphorylation levels of CREB (red) in PC12 cells. Treatment with 250 μM MGO for 1 h induced the phosphorylation of CREB, while preincubating the PC12 cells with K252a for 30 min blocked this effect. DAPI (blue) was employed to stain the nuclei. (***D***) Flag-tagged and His-tagged TrkBs were co-transfected into HEK-293 cells. The cells were then treated with either PBS, 250 μM MGO or 100 ng/mL BDNF for 30 min. Subsequently, Flag-tagged TrkB was pulled down and monitored by 6×His-tagged antibody. (***E***) Biolayer interferometry (BLI) data depicting the association and dissociation sensograms at different concentrations of MGO for the interaction analysis of MGO with the extracellular domain (ECD) of TrkB.

Figure 3. The antidepressant effects of MGO on CUMS rats. (***A***) Comparison of immobility time in the forced swim test (FST) of normal rats (control) and CUMS rats treated with either vehicle or MGO 5 mM/kg intraperitoneal (ip) per day for 3 weeks. MGO treatment significantly decreased the immobility time compared to CUMS rats. (***B***) In the elevated plus-maze

(EPM) test, CUMS rats exhibited decreased number of entries to open arms, whereas treating with MGO 5 mM/kg ip per day for 3 weeks significant increased the entry times to open arms. Data in ***A*** and ***B*** are presented as mean ± s.e.m., n = 10 per group. *P < 0.05, **P < 0.01, ***P < 0.001; one-way ANOVA with Dunnett's multiple comparisons test. (***C***) LC-MS/MS analysis of the concentrations of monoamines and their metabolites in the HC homogenates in rats. 5-HT, serotonin; DA, dopamine; 5-HIAA, 5-hydroxyindoleacetic acid; DOPAC, 3,4-dihydroxyphenylacetic acid; HVA, homovanillic acid. Data are presented as mean ± s.e.m., n = 5 per group. *P < 0.05, **P < 0.01, ***P < 0.001, NS = not significant; one-way ANOVA with Dunnett's multiple comparisons test. (***D***) Quantification of GLO1 protein levels (percentage of protein to GAPDH) in the HC and PFC of normal rats (control) and CUMS rats treated with either vehicle or MGO (5 mM/kg, ip) per day for 3 weeks. Data are presented as mean percentage ± s.e.m. of the mean values of the control group, n = 4 per group. *P < 0.05, NS = not significant; one-way ANOVA with Dunnett's multiple comparisons test. (***E***) MGO levels in the HC and PFC of normal rats (control) and CUMS rats treated with either vehicle or MGO (5 mM/kg, ip) per day for 3 weeks. MGO levels were measured by MGO-H1 protein adducts using ELISA assay. Data are presented as mean ± s.e.m., n = 5 per group. *P < 0.05, ***P < 0.001; one-way ANOVA with Dunnett's multiple comparisons test. (***F***) Western blotting analysis of GLO1, BDNF and other proteins involved in TrkB signaling pathway of HC lysates of different groups of rats. Compared to CUMS rats, MGO-treated rats (5 mM/kg, ip per day for 3 weeks) exhibited increased p-TrkB, p-Akt, p-ERK1/2 and p-CREB immunoreactivity (n = 4). (***G***) Heatmap showing the differentially expressed genes (DEGs) and enriched GO terms in the PFC of different groups of rats. (***H***) qRT-PCR analysis of the genes in TrkB signaling or genes related to cell proliferation in the PFC lysates of different group of rats. Data are presented as mean ± s.e.m., n = 5 per group. *P < 0.05, **P < 0.01, ***P < 0.001, NS = not significant; one-way ANOVA with Dunnett's multiple comparisons test. (***I***) Representative images of immunostaining of BrdU (red) and NeuN (green) in hippocampal dentate gyrus of rats, scale bar = 50 μm (left). The numbers of BrdU+ and BrdU+/NeuN+ cells are shown in right. MGO treatment increased the density of both BrdU+ new born neurons and BrdU+/NeuN+ neurons in the hippocampal dentate gyrus of CUMS rats. Data are presented as mean ± s.e.m., n = 5 per group. *P < 0.05, **P < 0.01; one-way ANOVA with Dunnett's multiple comparisons test.

Figure 4. Luteolin shows antidepressant effects through targeting GLO1. (***A***) Chemical structures of luteolin and its derivative lutD used in this study. (***B***) Fluorescence spectra analysis of GLO1 in the presence of various concentrations of luteolin. T = 298 K, λex = 280 nm, C_{GLO1} = 5 μM. (***C***) Representative western blot of CETSA (top) or CETSA melt curves (bottom) in cell lysate for GLO1 targeted by luteolin (at 100 μM). Data are presented as mean ± s.e.m., n = 3 samples collected independently. *P < 0.05, ***P < 0.001; two-way ANOVA with Sidak's multiple comparisons test between luteolin treatment group and DMSO group. (***D***) Plot view of MD-simulated binding mode of GLO1 with luteolin. (***E***) Drug affinity responsive target stability (DARTS) analysis that shows interactions between luteolin and GLO1 wild type or mutant. (***F*** and ***G***) Luteolin (10 mg/kg) significantly increased the number of entries of rats in central and open zones during the FST test (***F***) and decreased immobility time in the EPM test (***G***) compared to vehicle treatment, indicating an antidepressant-like response. Data in ***F*** and ***G*** are presented as mean ± s.e.m., n = 10 per group. *P < 0.05, **P < 0.01, ***P < 0.001, NS = not significant; one-way ANOVA with Dunnett's multiple comparisons test. (***H***) Plasma MGO levels of CUMS rats after treated with luteolin for 3, 12, 24 h. Data are presented as mean ± s.e.m., n = 5 per group. **P < 0.01, ***P < 0.001; one-way ANOVA with Dunnett's multiple comparisons test between CUMS+SAL group and other groups. (***I***) Time course of TrkB, Akt, ERK1/2 and CREB and their phosphorylation levels as assessed by western blot in the HC of CUMS rats after single dose treatment with luteolin (20 mg/kg) (n = 3).

565 **Figure 5. The molecular mechanisms underlying the antidepressant effects of MGO.** Under normal conditions, MGO
566 binds to the extracellular domain of TrkB and provokes its dimerization and autophosphorylation, which then activates the
567 downstream Akt and ERK signaling, as well as the phosphorylation of the transcription factor CREB. This effectively induces
568 the expression of BDNF and forms a BDNF-positive feedback loop, which further promotes the proliferation of neurons.
569 Whereas under depressive state, the concentrations of MGO are significantly decreased partly due to the increased
570 expression levels or enzyme activities of GLO1. This results in inactivation of the BDNF/TrkB signaling (left). GLO1 inhibitors,
571 such as luteolin, effectively increase the concentrations of MGO and thus exert antidepressant effects (right).

572

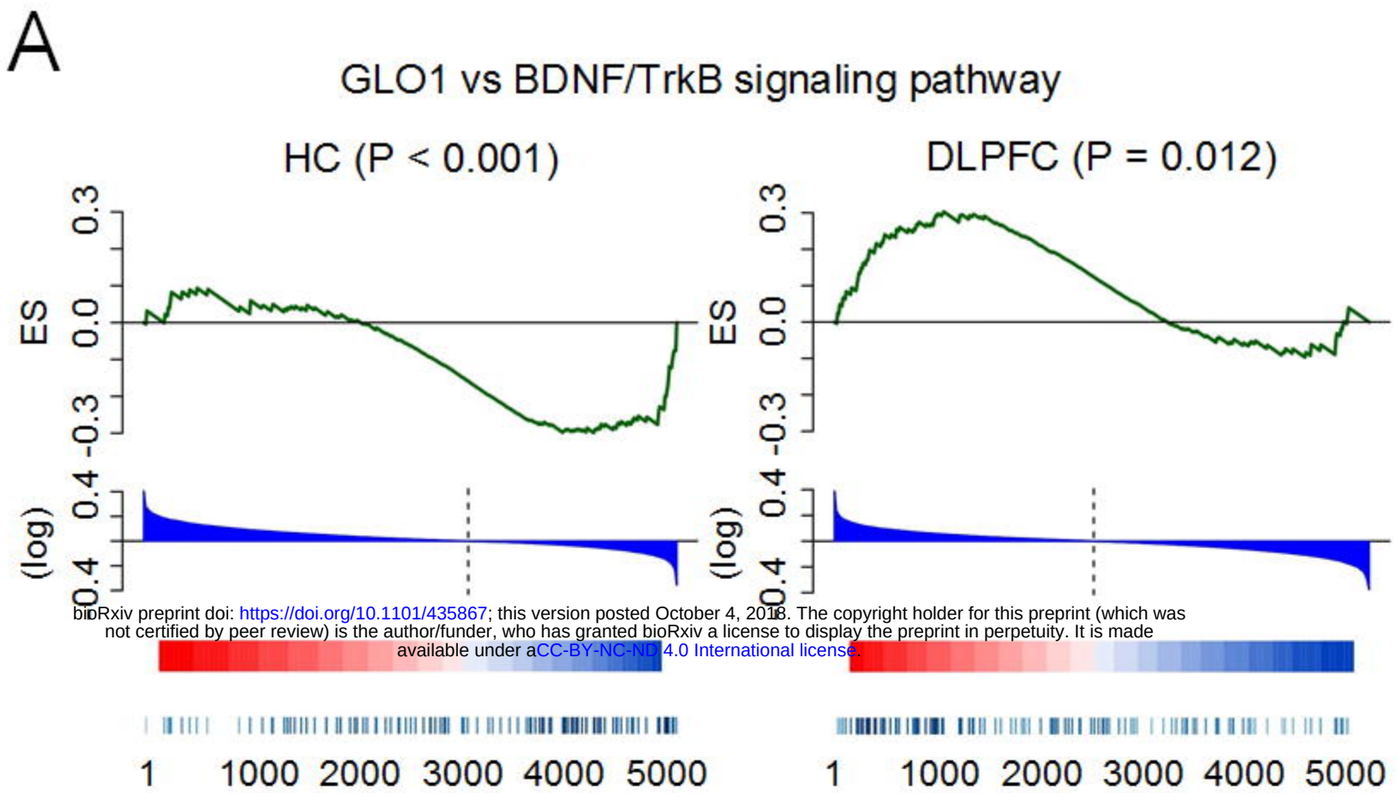

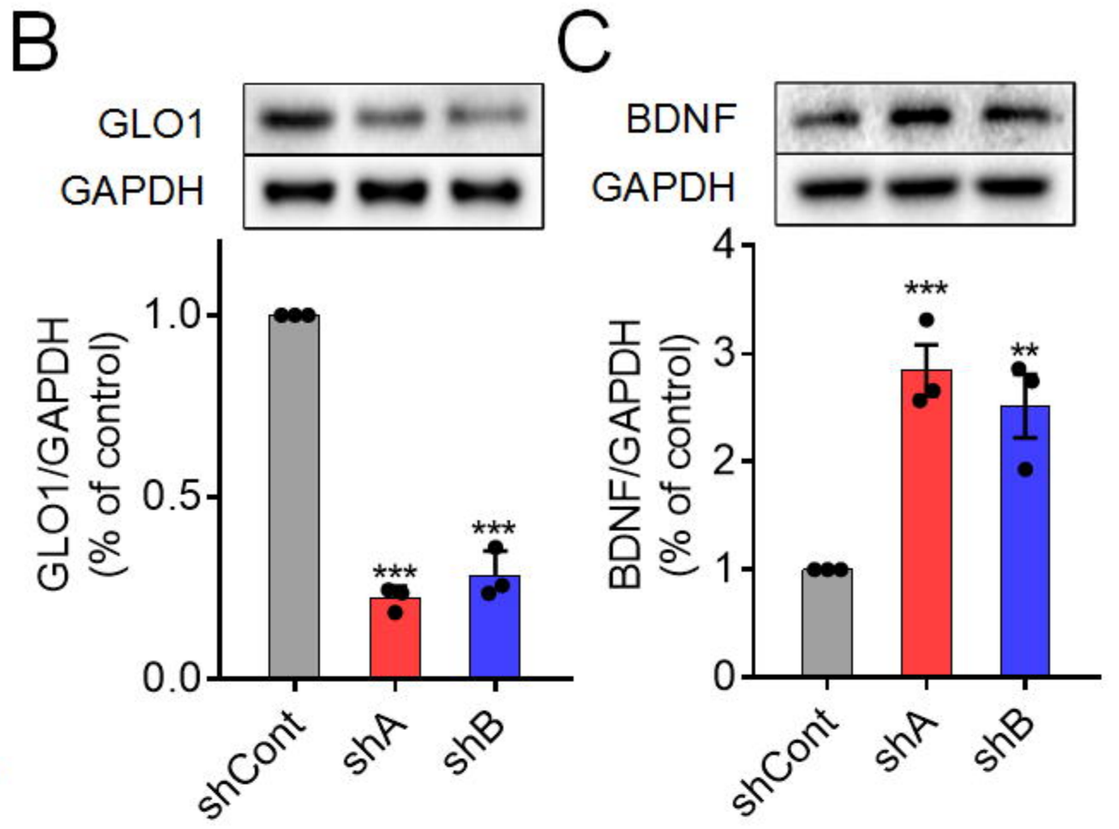

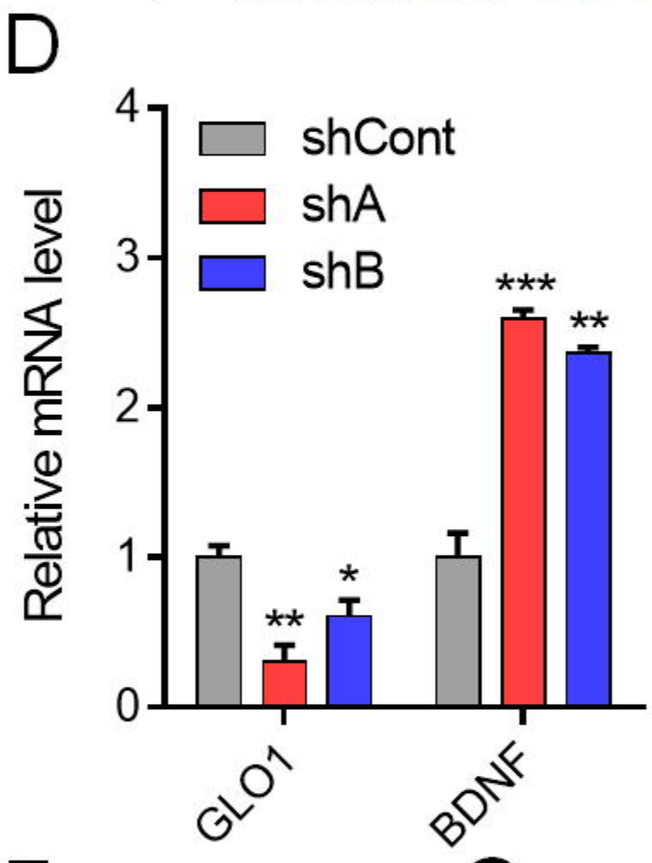

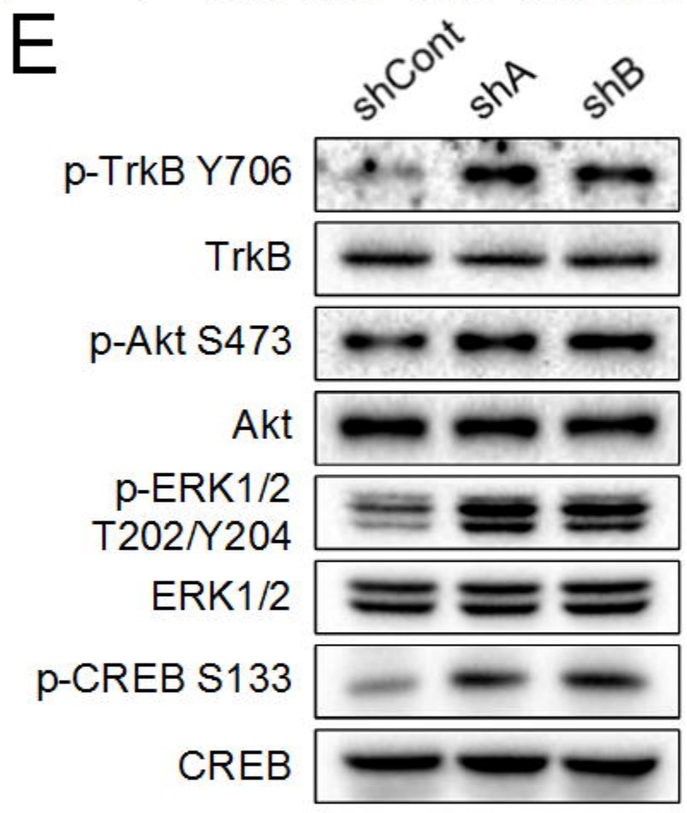

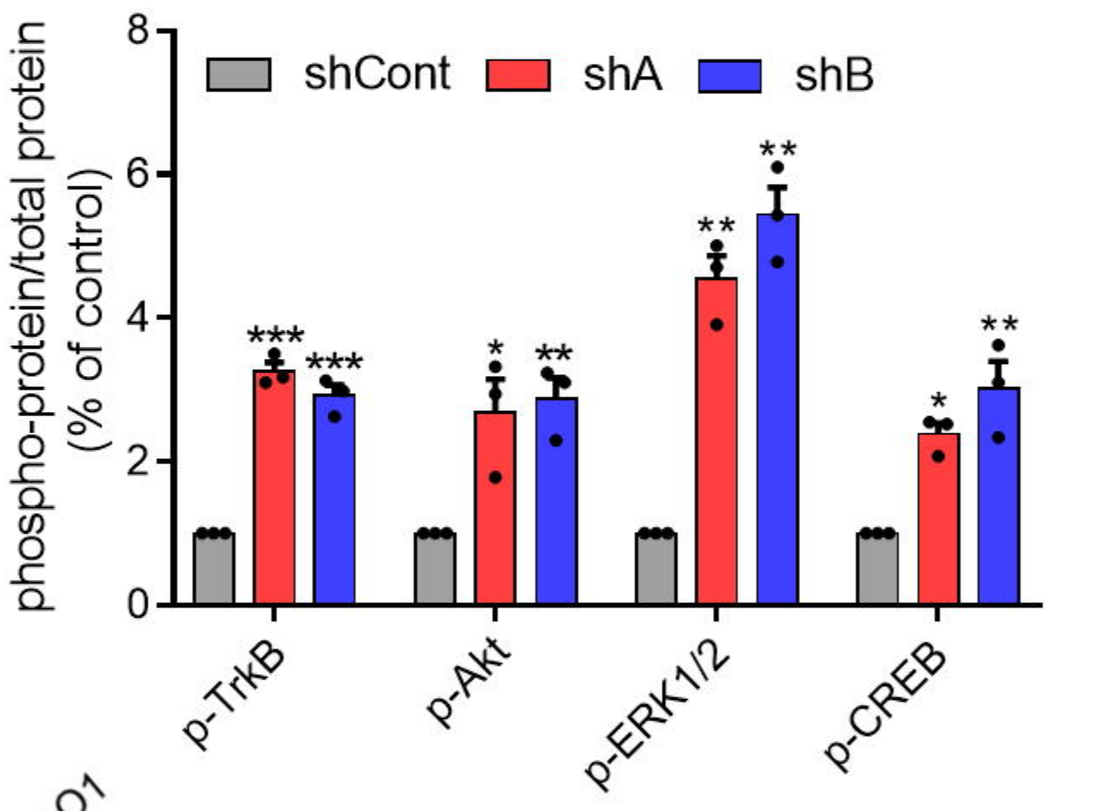

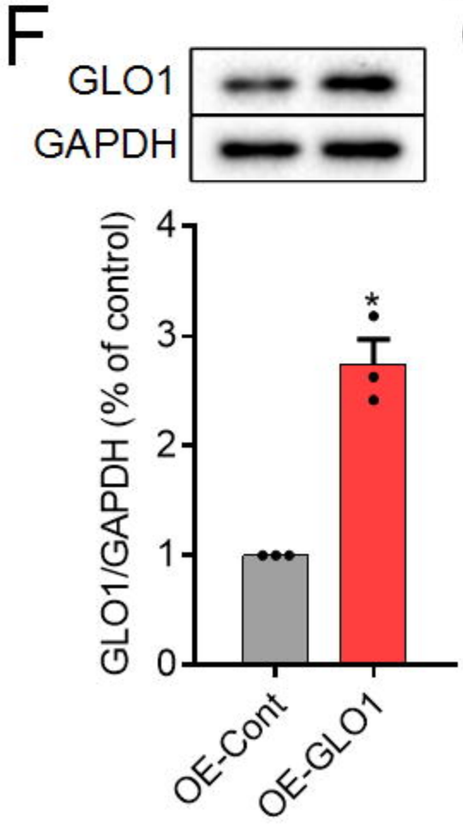

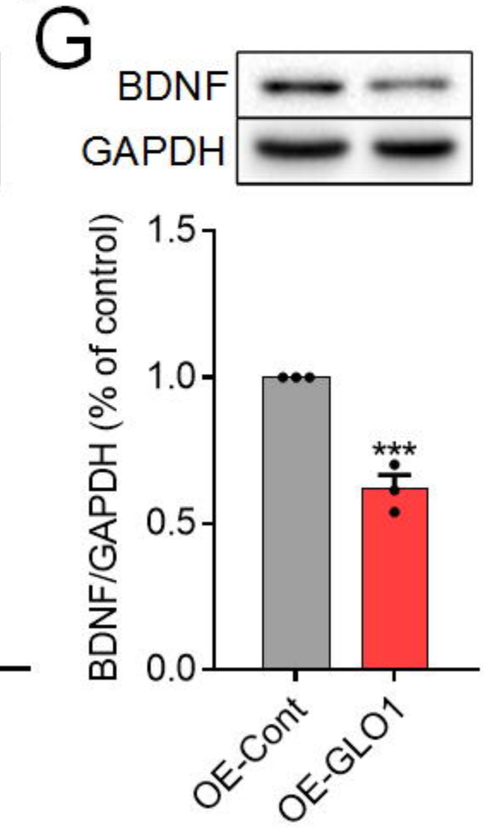

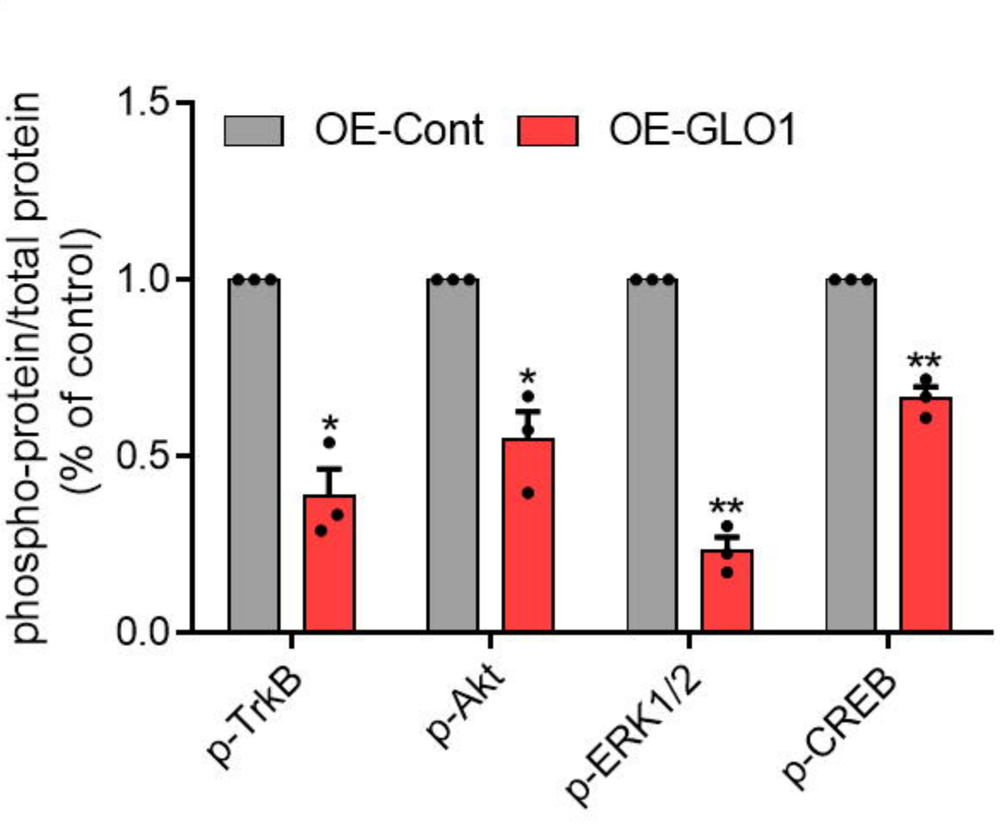

A

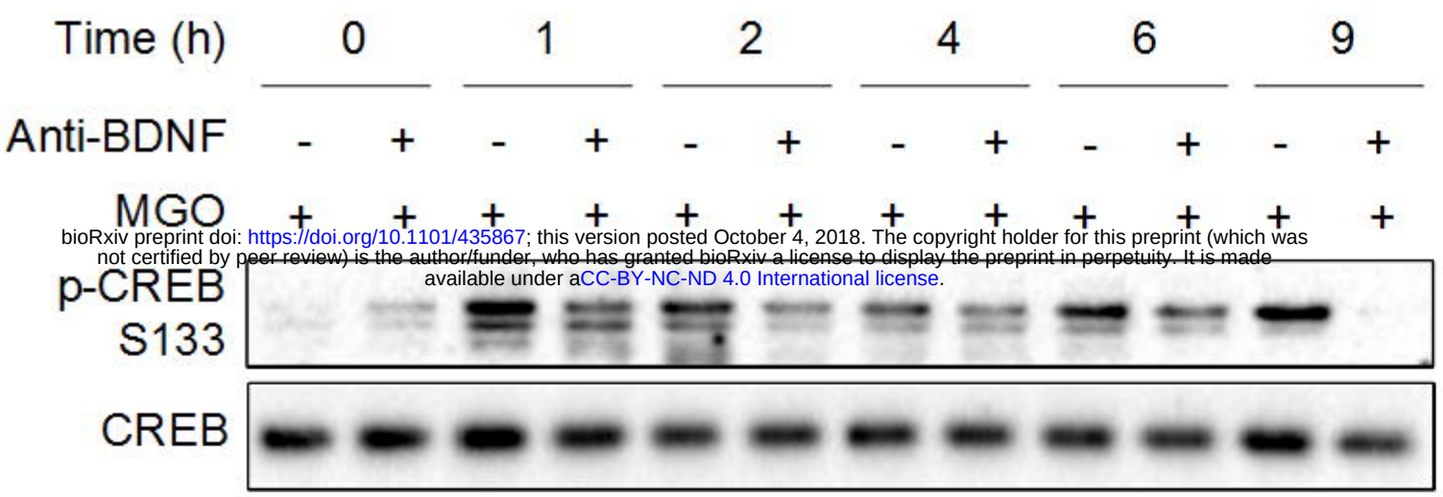

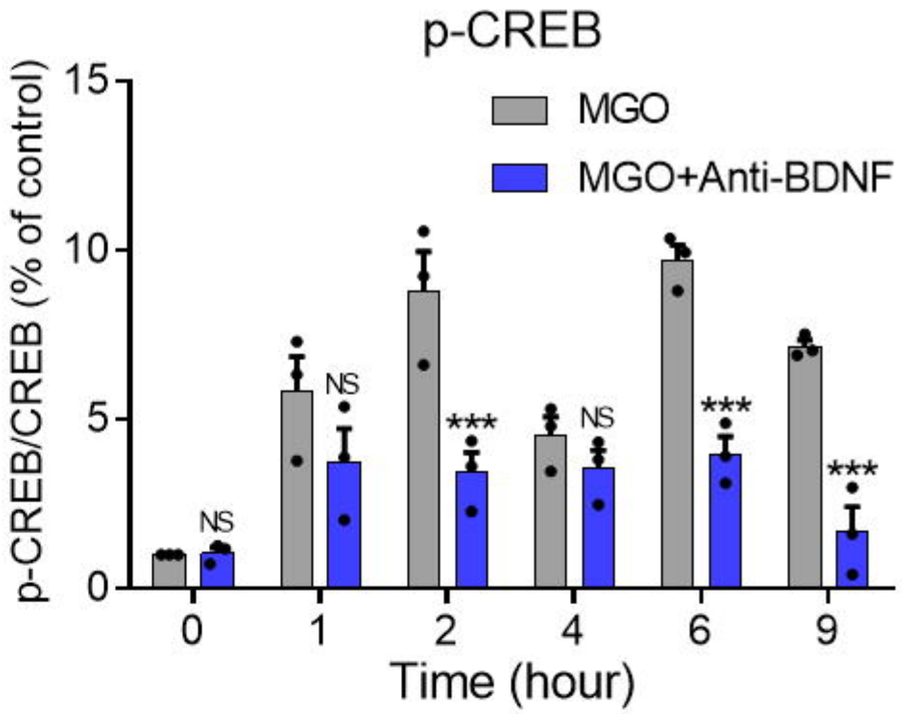

B

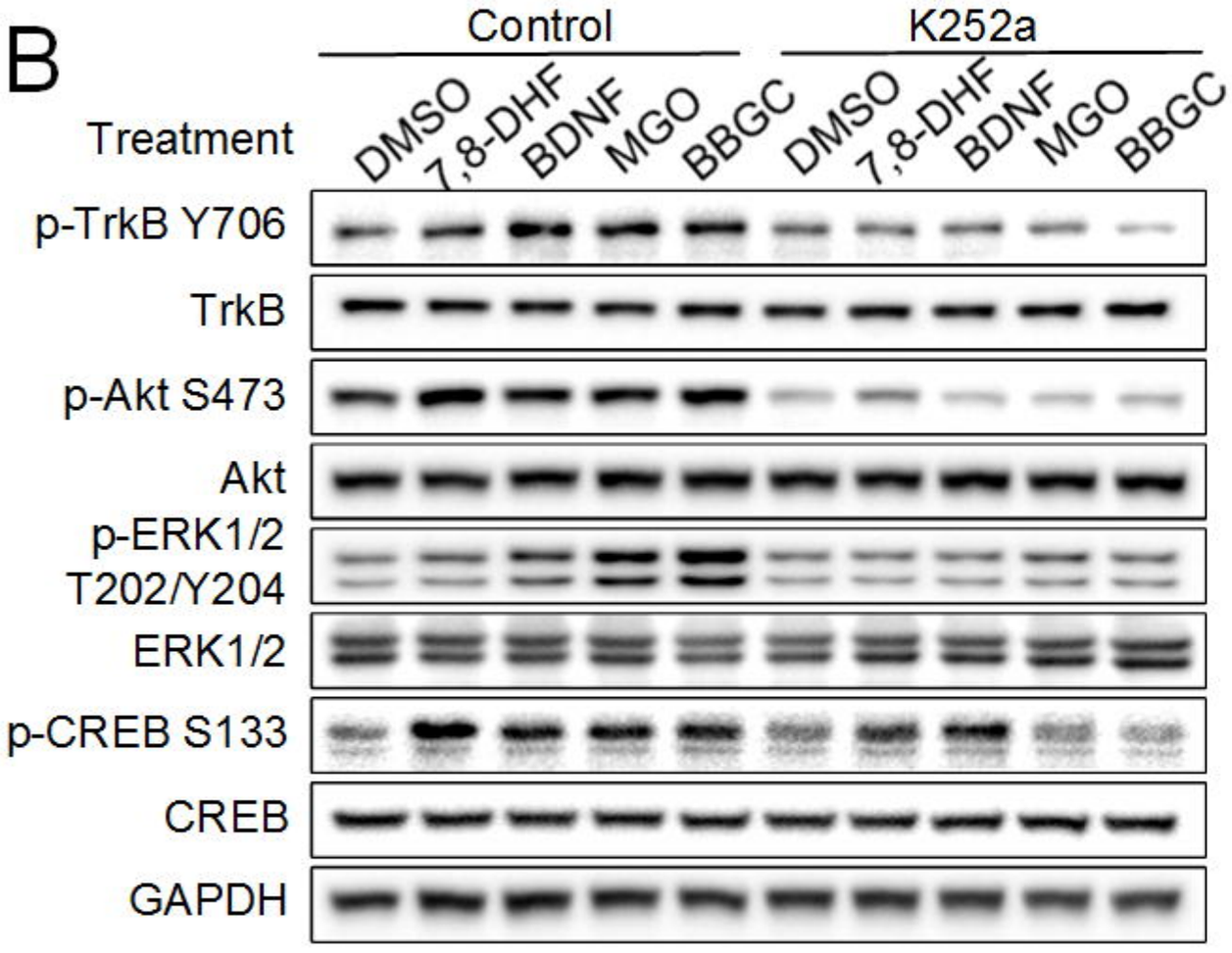

C

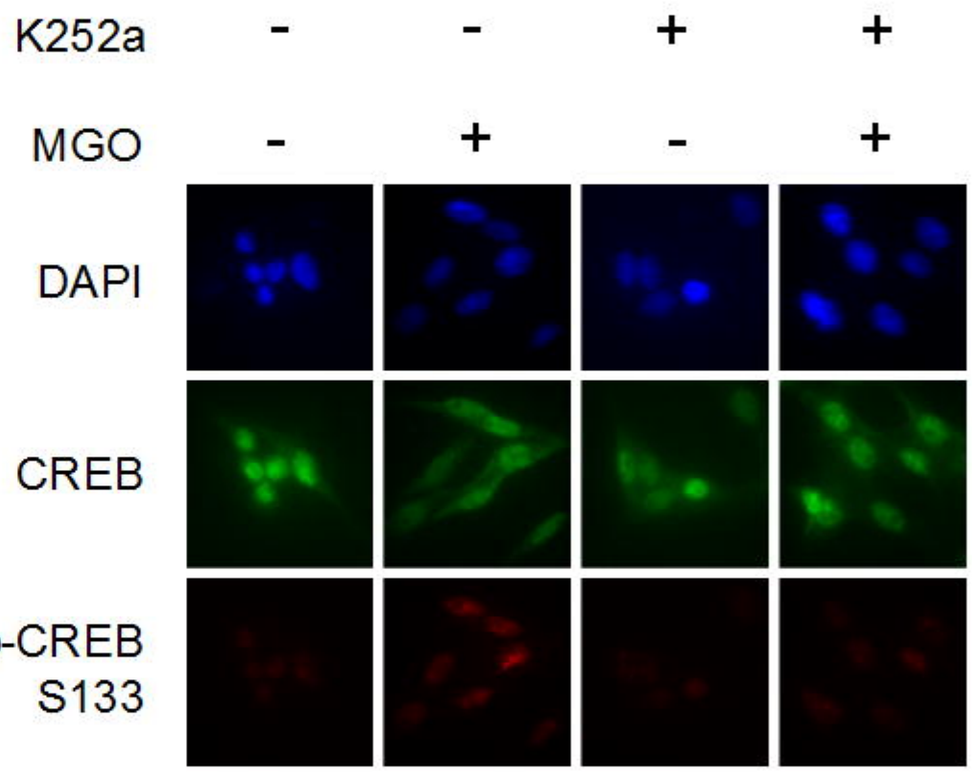

D

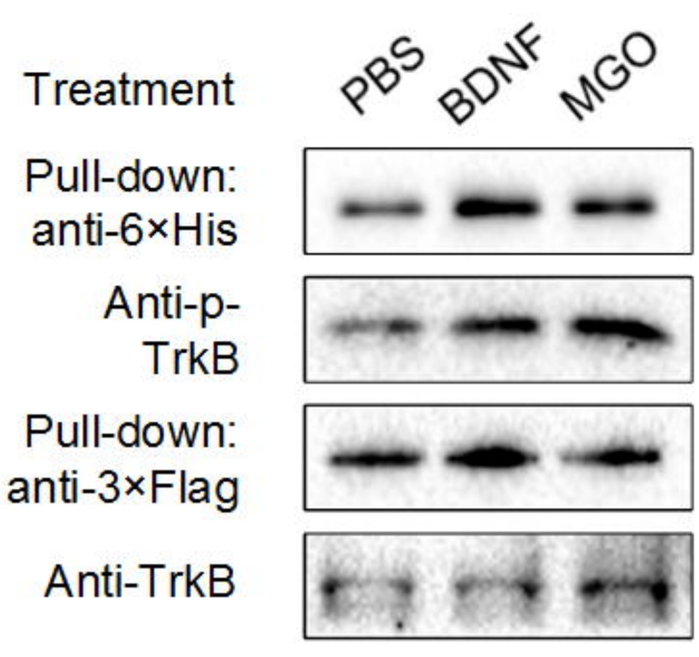

E

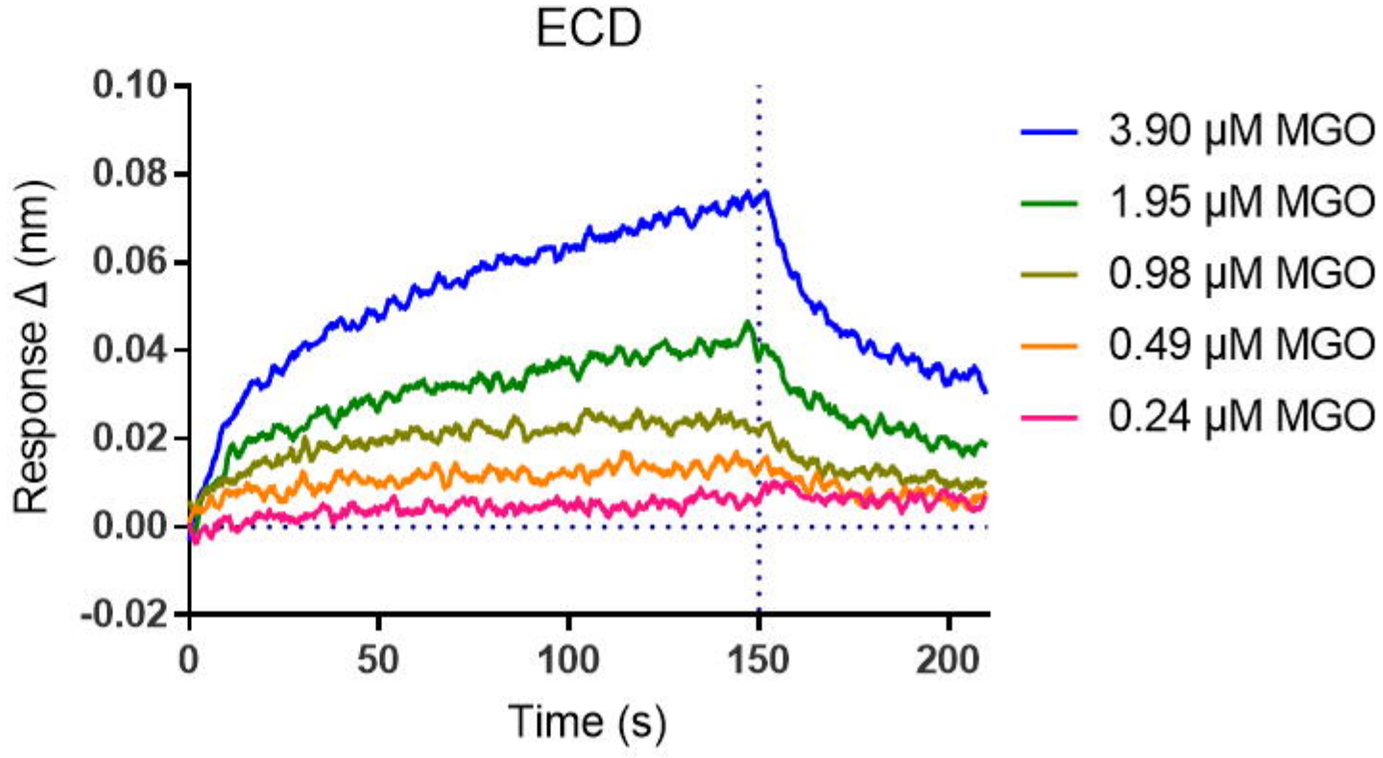

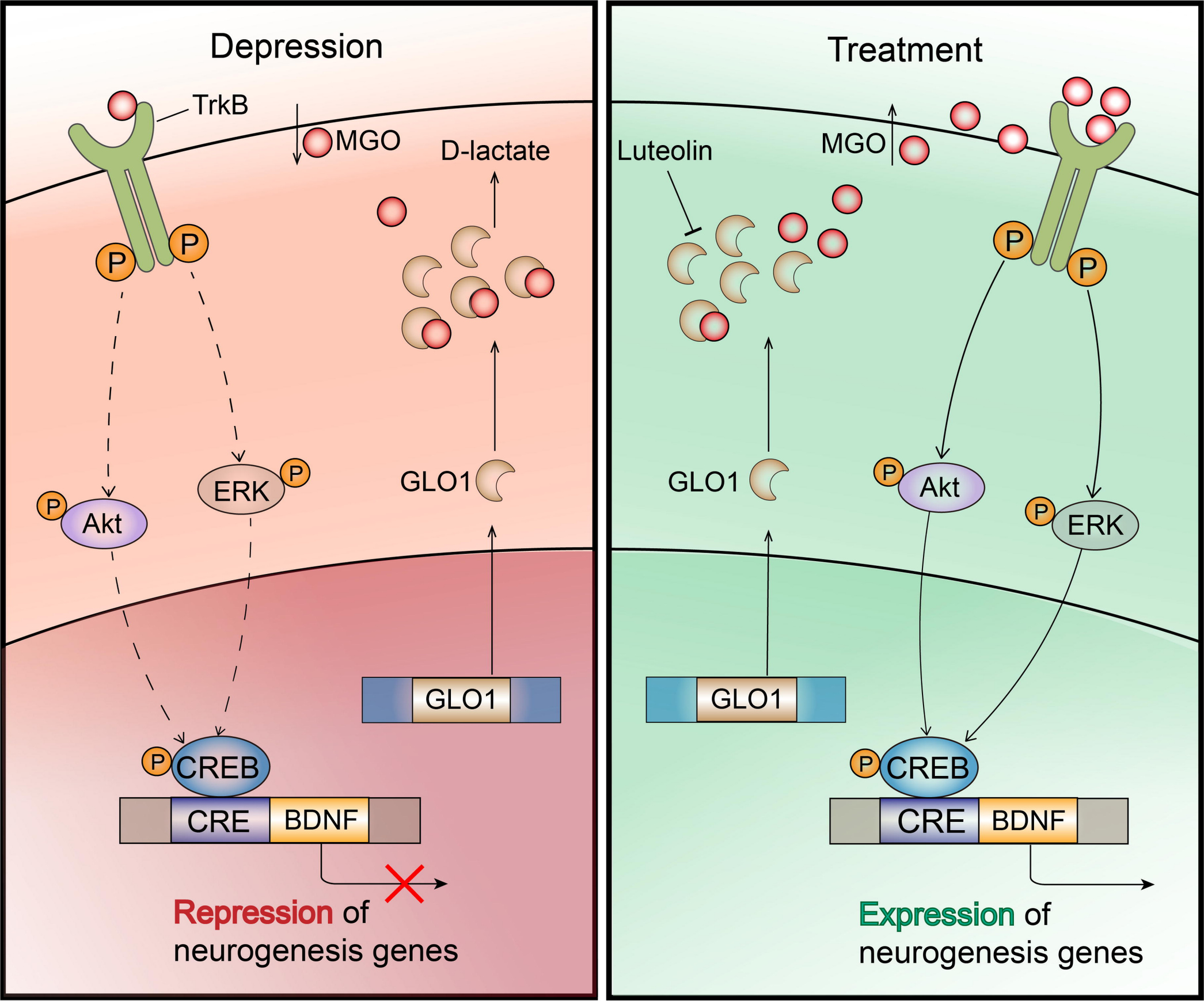
Depression
TrkB
MGO
D-lactate
P
P
P
Akt
ERK
P
GLO1
GLO1
P
CREB
CRE
BDNF
Repression of
neurogenesis genes
Treatment
Luteolin
MGO
P
P
GLO1
P
Akt
P
ERK
GLO1
P
CREB
CRE
BDNF
Expression of
neurogenesis genes